

ASXL1 mutations are associated with a response to alvocidib and 5-azacytidine combination in myelodysplastic neoplasms

Vladimir Riabov,¹ Qingyu Xu,¹ Nanni Schmitt,¹ Alexander Streuer,¹ Guo Ge,² Lyndsey Bolanos,³ Mark Wunderlich,³ Johann-Christoph Jann,¹ Alina Wein,¹ Eva Altmann,¹ Marie Demmerle,¹ Sanjay Mukherjee,⁴ Abdullah Mahmood Ali,⁴ Felicitas Rapp,¹ Verena Nowak,¹ Nadine Weimer,¹ Julia Obländer,¹ Iris Palme,¹ Melda Göl,¹ Ahmed Jawhar,⁵ Ali Darwich,⁵ Patrick Wuchter,⁶ Christel Weiss,⁷ Azra Raza,⁴ Jason M. Foulks,⁸ Daniel T. Starczynowski,^{3,9} Feng-Chun Yang,² Georgia Metzgeroth,¹ Laurenz Steiner,¹ Mohamad Jawhar,¹ Wolf-Karsten Hofmann¹ and Daniel Nowak¹

¹Department of Hematology and Oncology, Medical Faculty Mannheim, Heidelberg University, Mannheim, Germany; ²Department of Cell Systems & Anatomy, University of Texas Health Science Center at San Antonio, San Antonio, TX, USA; ³Division of Experimental Hematology and Cancer Biology, Cincinnati Children's Hospital Medical Center, Cincinnati, OH, USA; ⁴Myelodysplastic Syndromes Center, Columbia University Irving Medical Center, Columbia University, New York, NY, USA; ⁵Department of Orthopedic Surgery, Medical Faculty Mannheim, Heidelberg University, Mannheim, Germany; ⁶Institute of Transfusion Medicine and Immunology, German Red Cross Blood Service Baden-Württemberg-Hessen, Medical Faculty Mannheim, Heidelberg University, Mannheim, Germany; ⁷Department of Medical Statistics, Biomathematics and Information Processing, Medical Faculty Mannheim, Heidelberg University, Mannheim, Germany; ⁸Sumitomo Pharma Oncology, Inc., Lehi, UT, USA and ⁹University of Cincinnati Cancer Center, Cincinnati, OH USA

Correspondence: D. Nowak
daniel.nowak@medma.uni-heidelberg.de

V. Riabov
vladimir.ryabov@medma.uni-heidelberg.de

Received: February 9, 2023.

Accepted: October 24, 2023.

Early view: November 2, 2023.

<https://doi.org/10.3324/haematol.2023.282921>

©2024 Ferrata Storti Foundation

Published under a CC BY-NC license



Supplementary Methods

Isolation of MNCs and CD34+ HSPCs from BM aspirates and bone specimens

Mononuclear cells (MNCs) were isolated using Ficoll-Paque (Cytiva, 17-5442-03) density gradient centrifugation. CD34⁺ HSPCs enrichment from MNCs was performed using MACS columns (Miltenyi Biotec, 130-046-703).

HSPCs cultures and cell viability assays

To generate dose-response curves using CellTiter-Glo (CTG) assay (Promega, G7571), 2.5×10^3 cells from n=12 HC and n=16 MDS patients were treated with alvocidib for 24h, 5-AZA for 48h or DMSO for 24h or 48h (controls) in 50 μ l of the medium. Cell viability data for each patient were normalized to its own untreated control (DMSO). Median IC30 concentrations of 5-AZA (254 nM) and alvocidib (90 nM) were calculated from dose-response curves for MDS patient samples. For combination treatment, HSPCs of all n=45 MDS patients and n=11 HC were treated with IC30 concentrations of 5-AZA (48h) followed by alvocidib treatment for 24h. CTG assays were performed after 72h according to the manufacturer's instructions. The luminescent signal was measured using a Tecan Infinite F200 Pro Microplate Reader.

For apoptosis assays, expanded human HSPCs (1×10^5) were treated in a 300 μ l medium with IC30 concentrations of both drugs as indicated above for the CTG assays. In some of the experiments, expanded HSPCs were treated with BH3 mimetics ABT-199, S-63845 and A1331852 (all from Selleckchem) for 24h. The concentrations of BH3 mimetics are indicated on the graphs. The percentages of apoptotic (Annexin V⁺ SYTOX Green⁻) and apoptotic+dead cells (Annexin V⁺SYTOX Green⁻ + Annexin V⁺SYTOX Green⁺ + Annexin V⁻SYTOX Green⁺) were determined using the Dead Cell Apoptosis Kit with Annexin V APC and SYTOX Green (ThermoFisher Scientific, V35113) according to the manufacturer's instructions. A fluorescent signal was detected using BD FACSCelesta flow cytometer or BD FACS Melody flow cytometer/sorter.

CTG assays for mouse cells were performed as follows: Frozen whole bone marrow cells (1×10^5 in 150 μ l medium) were thawed and immediately treated with indicated concentrations of alvocidib and 5-AZA for 8h. Both drugs were added simultaneously.

Myeloid panel sequencing

DNA was isolated using the AllPrep DNA/RNA mini or micro Kit or QIAamp DNA Micro Kit (Qiagen, 56304). For panel deep sequencing, 250ng of genomic DNA from patient samples was subjected to the Nextera DNA Flex Kit with the usage of unique dual indices. The enrichment was performed using the IDT Hybridization Capture protocol and a corresponding custom myeloid panel (IDT, Integrated DNA Technologies, Coralville, IA, USA) including the following recurrently mutated MDS-related genes: *ASXL1*, *ASXL2*, *ATRX*, *BCOR*, *BCORL1*, *BRAF*, *BRCC3*, *CALR*, *CBL*, *CDH23*, *CDKN2A*, *CEBPA*, *CREBBP*, *CSF3R*, *CSNK1A1*, *CTCF*, *CUX1*, *DDX41*, *DDX54*, *DHX29*, *DNMT3A*, *EP300*, *ETNK1*, *ETV6*, *EZH2*, *FLT3*, *GATA1*, *GATA2*, *GNAS*, *GNB1*, *IDH1*, *IDH2*, *JAK2*, *KDM5A*, *KDM6A*, *KIT*, *KMT2D*, *KRAS*, *MPL*, *MYC*, *NF1*, *NPM1*, *NRAS*, *PHF6*, *PIGA*, *PPM1D*, *PRPF8*, *PTPN11*, *RAD21*, *RUNX1*, *SETBP1*, *SF1*, *SF3A1*, *SF3B1*, *SH2B3*, *SMC1A*, *SMC3*, *SRSF2*, *STAG2*, *SUZ12*, *TET2*, *TP53*, *U2AF1*, *U2AF2*, *WT1*, *ZBTB7A*, *ZRSR2*. The final library pools were sequenced on a S4 Nova Seq Flow Cell (Illumina) with 150 bp paired-end reads. The mean sequencing depth was 1430.199-fold. Bioinformatical processing consisted of quality trimming using Seqtk (version 1.2) and was followed by a comprehensive quality control using the FastQC package (version 0.11.5). The following criteria were applied to filter relevant variants: only exonic and splicing variants (unless there is an entry in "pathogen" in CLINSIG database), synonymous variants were excluded, no snp137 entry (unless there is an entry in "pathogen" in CLINSIG database), PopFreqMax < 0.1 (unless there is an entry in "pathogen" in CLINSIG database). Myeloid panel sequencing data have been deposited in the EGA archive (Accession code: EGAS00001007007). Access can be requested via EGA, but also by direct personal communication with the corresponding authors of the manuscript.

MCL-1 dependency assay

Frozen MNCs were incubated for 1h, 37°C in RPMI 1640 medium + 10% FBS + 5 µl/ml DNase I (Stem Cell Technologies, 07900). Subsequent labeling of the cells with antibody mix, treatment with MCL-1 antagonistic peptide T-MS1 or water (control) and mitochondrial stainings were performed using T-MS1 Based MCL-1 Dependency Assay as described previously (1). Percent of mitochondrial priming in CD45^{dim}CD7⁺CD34⁺CD117⁺ blasts after T-MS1 treatment was calculated as follows: % Priming = (Average % Polarized Water - % Polarized Peptide)/(Average % Polarized Water)×100. Calibrated % Priming = Average % Priming ×1.6 as described previously (1). Samples were acquired using BD FACSAria IIu flow cytometer/sorter.

CFU assay

CD34+ BM cells of n=5 MDS patients were treated with IC30 concentrations of 5-AZA (48h), alvocidib (24h) or 5-AZA (48h) followed by alvocidib (24h) in StemSpan™ SFEM II medium supplemented with recombinant human (rh) stem cell factor (rhSCF, Stemcell Technologies, 78062, 50ng/ml), rh fibroblast growth factor-1 (Thermofisher scientific, 13241-013, 10ng/ml), rh fms-like tyrosine kinase 3/fetal liver kinase-2 ligand (Stemcell Technologies, 78137, 50ng/ml) and rh thrombopoietin (Stemcell Technologies, 78210, 10ng/ml) . In vitro expansion of CD34+ cells was not performed in order to keep stemness of CD34+ cells. After treatment, CD34+ cells were seeded into semi-solid MethoCult H4435 Enriched Methylcellulose-based medium (Stemcell Technologies, H4435) at a density of 3000 cells/35mm dish in 1ml of medium. After incubation for 14 days (5% CO₂, 37°C), cells were harvested from CFU plates by centrifugation and analyzed by flow cytometry.

Cytological assessments

May-Grünwald-Giemsa stained cytopins prepared from BM MNCs were used for morphological analyses. Immature myeloid cells in the BM were identified and quantified in a blinded manner.

RNA isolation, cDNA synthesis and quantitative reverse transcription PCR (RT-qPCR)

RNA was isolated using the AllPrep DNA/RNA mini or micro Kit (Qiagen, 80204 or 80284 respectively). cDNA synthesis was performed using the QuantiTect Reverse Transcription kit (Qiagen, 205311). RT-qPCR for the analysis of *MCL-1* and *NOXA* gene expression was performed using a LightCycler 480 Instrument II (Roche Life Science) and LightCycler® 480 Probes Master mix (Roche Life Science, 04 887 301 001). Gene expression TaqMan assays Hs01050896_m1 for *MCL-1* and Hs00560402_m1 for *NOXA* (PMAIP1) were purchased from ThermoFisherScientific. Gene expression data were normalized to the expression of β -actin. Relative gene expression was calculated using the $2^{-\Delta\Delta C_t}$ method (2).

Statistical analysis

Statistical analysis was performed using GraphPad Prism 8.4.3 software (San Diego, CA, USA). The types of statistical tests are specified in figure legends or manuscript text. *P* values < 0.05 indicated statistical significance. Binomial logistic regression analysis was conducted for multivariable analyses based on IBM SPSS Statistics version 28 (Armonk, NY, USA). The following parameters were included in the logistic regression model as binary outcomes: age ≥ 70 vs. < 70 years, sex, IPSS-R int/high vs IPSS-R very high; *ASXL1*, *TET2*, *RUNX1*, *EZH2*, *ZRSR2*, and *STAG2* mutations with the following outcomes: 1 = presence of mutation, 0 = no mutation.

1. Zeidner JF, Lee DJ, Frattini M, Fine GD, Costas J, Kolibaba K, et al. Phase I Study of Alvocidib Followed by 7+3 (Cytarabine + Daunorubicin) in Newly Diagnosed Acute Myeloid Leukemia. Clin Cancer Res. 2021 Jan 1;27(1):60-9.
2. Livak KJ, Schmittgen TD. Analysis of relative gene expression data using real-time quantitative PCR and the $2^{-\Delta\Delta C(T)}$ Method. Methods (San Diego, Calif). 2001 Dec;25(4):402-8.

Supplementary Table 1. Individual patient characteristics

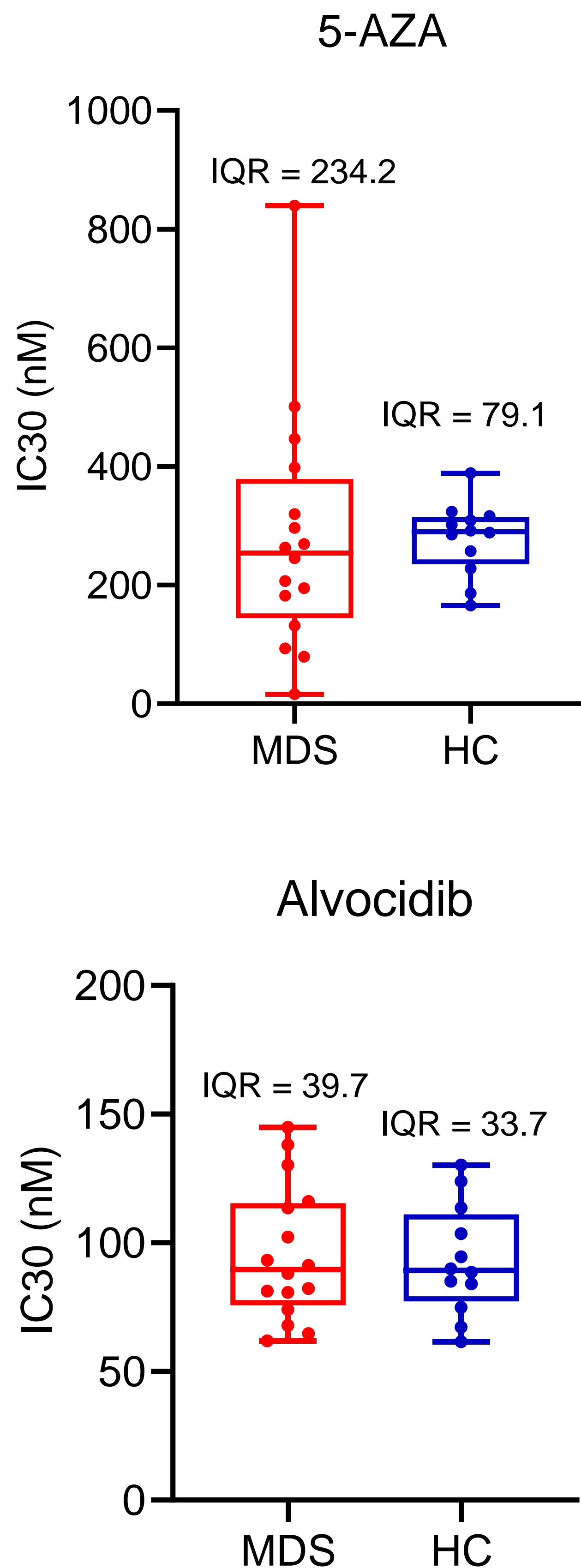
No.	Age, years	Sex	Subtype WHO 2016	IPSS-R	Mutations
P_01	55	m	MDS-EB2	high	NF1, PTPN11, TP53
P_02	71	m	MDS-EB2	high	ZRSR2, KMT2D, TET2, PHF6
P_03	79	m	MDS-EB1	high	ASXL1, TET2, RUNX1, STAG2, EZH2
P_04	70	m	MDS-MLD	high	ASXL1, TET2, RUNX1, STAG2, ZRSR2, EZH2, DHX29, NRAS, PTPN11
P_05	59	m	MDS-EB1	high	SF3B1, FLT3-ITD
P_06	82	m	MDS-EB2	very high	TP53, ZBTB7A
P_07	64	m	MDS-EB2	high	ASXL1, SRSF2, SETBP1, ETV6, NRAS
P_08	80	m	MDS-EB2	very high	TP53
P_09	72	m	MDS-EB2	very high	ASXL1, DNMT3A, U2AF1, IDH2
P_10	83	m	MDS-MLD	high	TP53
P_11	84	m	MDS-EB2	very high	TET2, RUNX1, EZH2, CUX1, ZBTB7A
P_12	76	m	MDS-EB2	very high	No mutations
P_13	86	w	MDS/MPN unclassifiable	high	SRSF2, CEBPA, CDH23, ASXL2
P_14	73	m	MDS-MLD	very high	KMT2D, TP53
P_15	69	m	MDS-EB2	intermediate	CUX1, DDX41
P_16	77	m	MDS-EB1	very high	ASXL1, SRSF2, STAG2
P_17	62	m	MDS-EB2	very high	DNMT3A
P_18	44	w	MDS-EB1	high	RUNX1, SF3B1, PTPN11
P_19	63	m	MDS-EB1	high	RUNX1, SRSF2, CREBBP, IDH1 , IDH2
P_20	64	w	MDS-EB2	very high	TP53, DNMT3A
P_21	74	m	MDS-EB2	high	TET2, BCOR, CDH23, U2AF1, BCORL1
P_22	73	m	AML-MRC	n.a.	SF3B1, RUNX1
P_23	82	w	MDS-MLD	high	TP53, DHX29
P_24	89	m	MDS-EB1	high	RUNX1, SF3B1, PHF6
P_25	72	m	MDS-EB2	high	ZRSR2, DDX41, EZH2
P_26	73	m	MDS-EB1	high	TET2, SF3B1
P_27	59	m	MDS-EB1	very high	TP53, CREBBP, DHX29
P_28	56	m	MDS-EB2	high	ASXL1, STAG2, ZRSR2, NF1, EZH2
P_29	72	m	MDS-EB1	high	ASXL1, TET2, RUNX1, STAG2, EZH2, ZRSR2
P_30	69	w	MDS/MPN unclassifiable	intermediate	ASXL1, TET2, SRSF2, SETBP1, CREBBP, EP300, CBL
P_31	80	w	MDS-EB2	high	TET2
P_32	76	m	MDS-EB2	very high	ASXL1, RUNX1, SRSF2, STAG2
P_33	74	w	MDS-EB2	very high	ASXL1, ZRSR2, JAK2
P_34	75	m	MDS-MLD	high	TET2
P_35	43	m	MDS/MPNu	high	ASXL1, TET2, RUNX1, ZRSR2, EZH2
P_36	73	m	sAML	n.a.	ASXL1, RUNX1, SRSF2, BCOR, SETBP1, PHF6, NRAS, IDH1
P_37	87	w	CMML-II	CPSS high	TP53, DNMT3A, CDH23
P_38	66	w	MDS-EB2	high	ASXL1
P_39	73	w	sAML	n.a.	TET2, CEBPA, BCOR, PHF6, BCORL1, DNMT3A, NRAS
P_40	90	m	AML-MRC	n.a.	BCOR, U2AF1, NRAS
P_41	76	w	MDS-EB2	high	ASXL1, CSF3R, RUNX1, SRSF2, TET2
P_42	78	m	MDS-RS-	intermediate	ASXL1, RUNX1, SRSF2, U2AF1,

			MLD		BCOR
P_43	73	m	MDS-EB2	intermediate	ASXL1, NF1, SETBP1, SRSF2, TP53, U2AF1
P_44	75	m	MDS-MLD	intermediate	EZH2, STAG2, TET2, ZRSR2
P_45	79	m	MDS-EB1	high	ASXL1, PHF6, RUNX1, U2AF1

Supplementary Table 2. Myeloid panel deep sequencing results of n=9 healthy control (HC) bone marrow specimens

HC ID	Age	Sex	Detected mutation
1	47	F	No
2	65	F	DNMT3A (W305fs), VAF = 33%
3	74	F	No
4	65	F	No
5	66	M	No
6	47	F	No
7	73	M	No
8	81	M	No
9	85	F	No

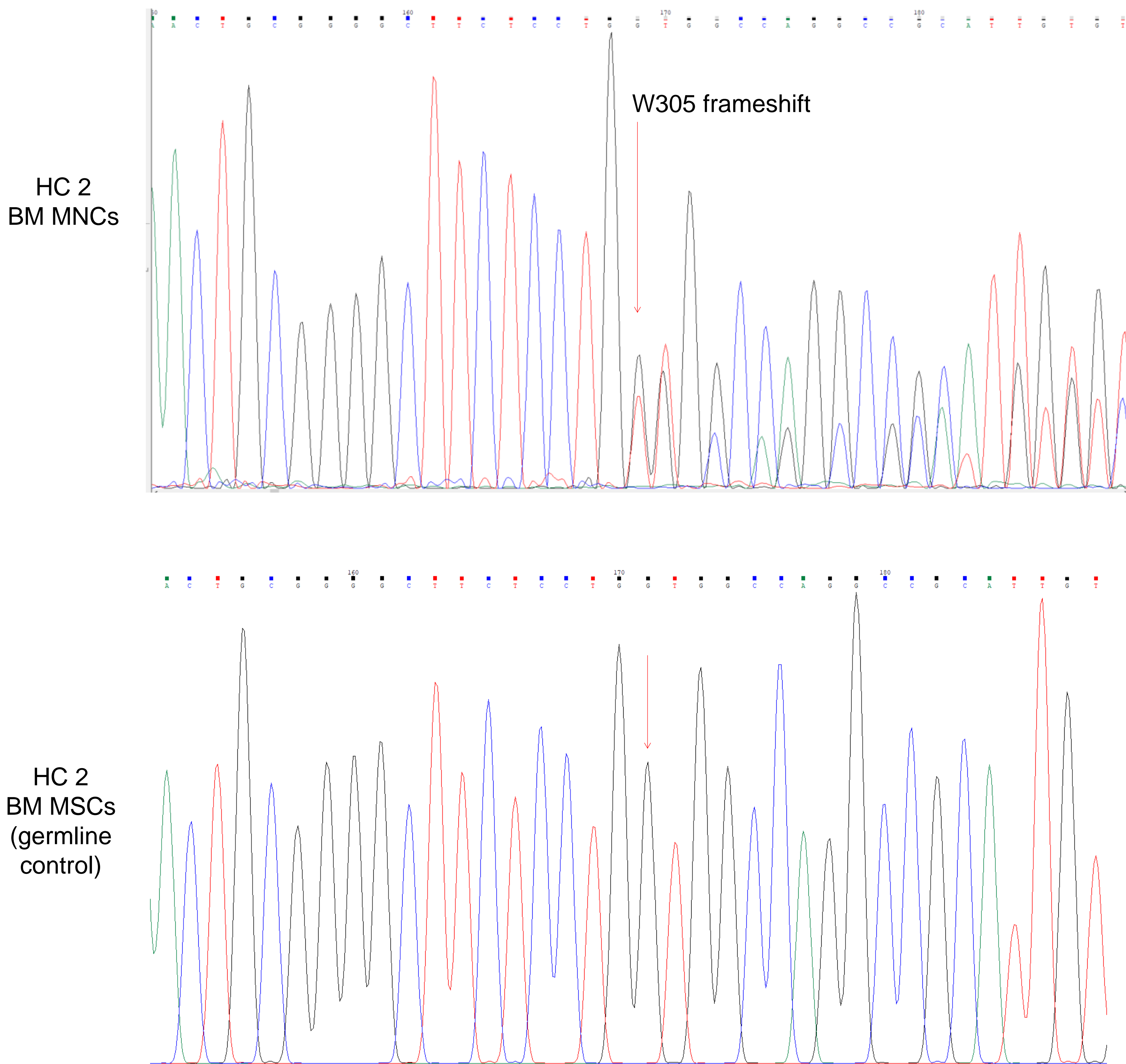
Figure S1



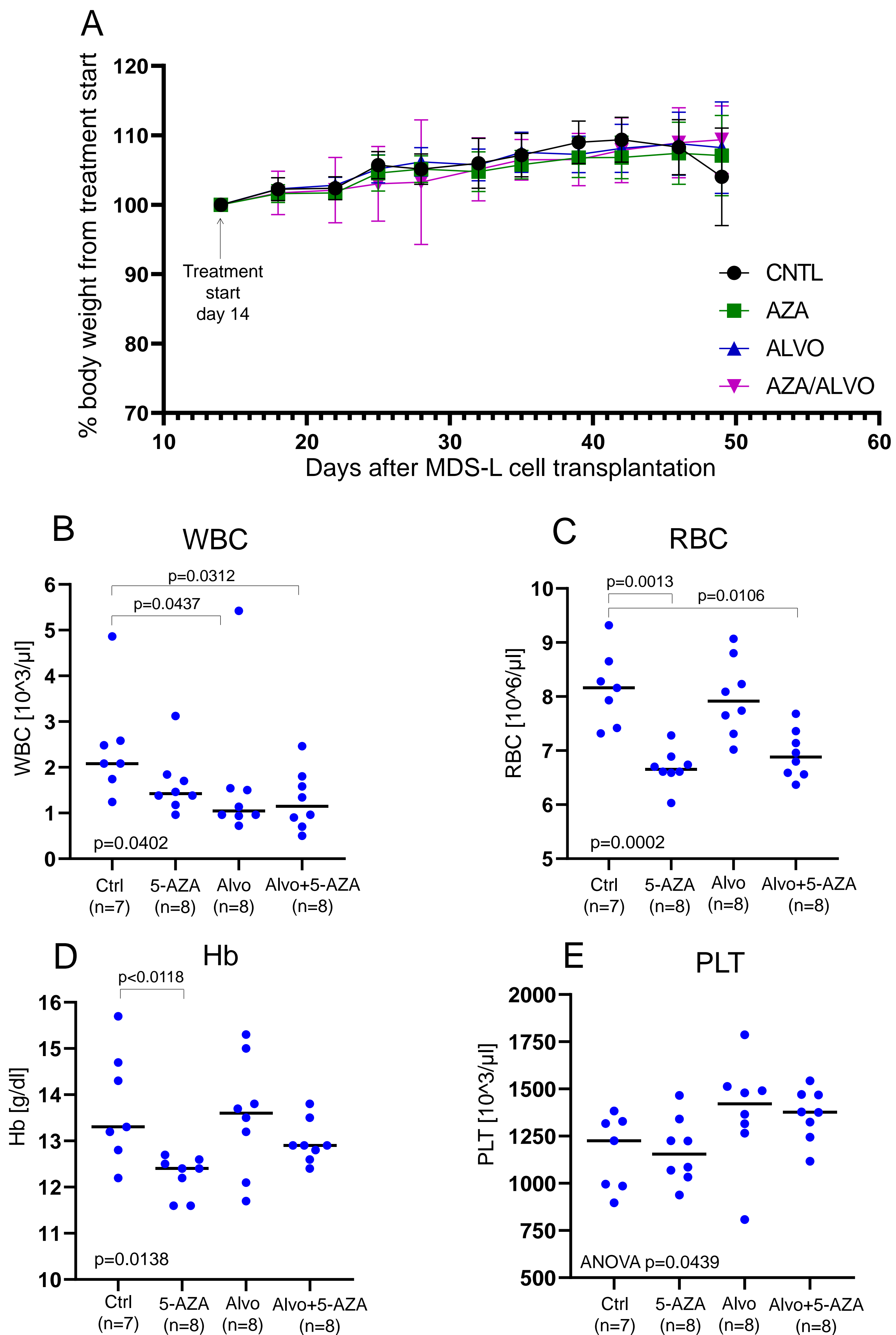
Supplementary Figure 1. Heterogenous 5-AZA sensitivity in MDS samples. IC30 values are shown after treatment of expanded CD34+ MDS cells (n=16) or CD34+ HC cells (n=12) using 5-AZA for 48h or alvocidib for 24h. The data are presented as boxplots with whiskers indicating Min and Max values. IQRs (nM) are indicated on the graphs.

Figure S2

DNMT3A sequence

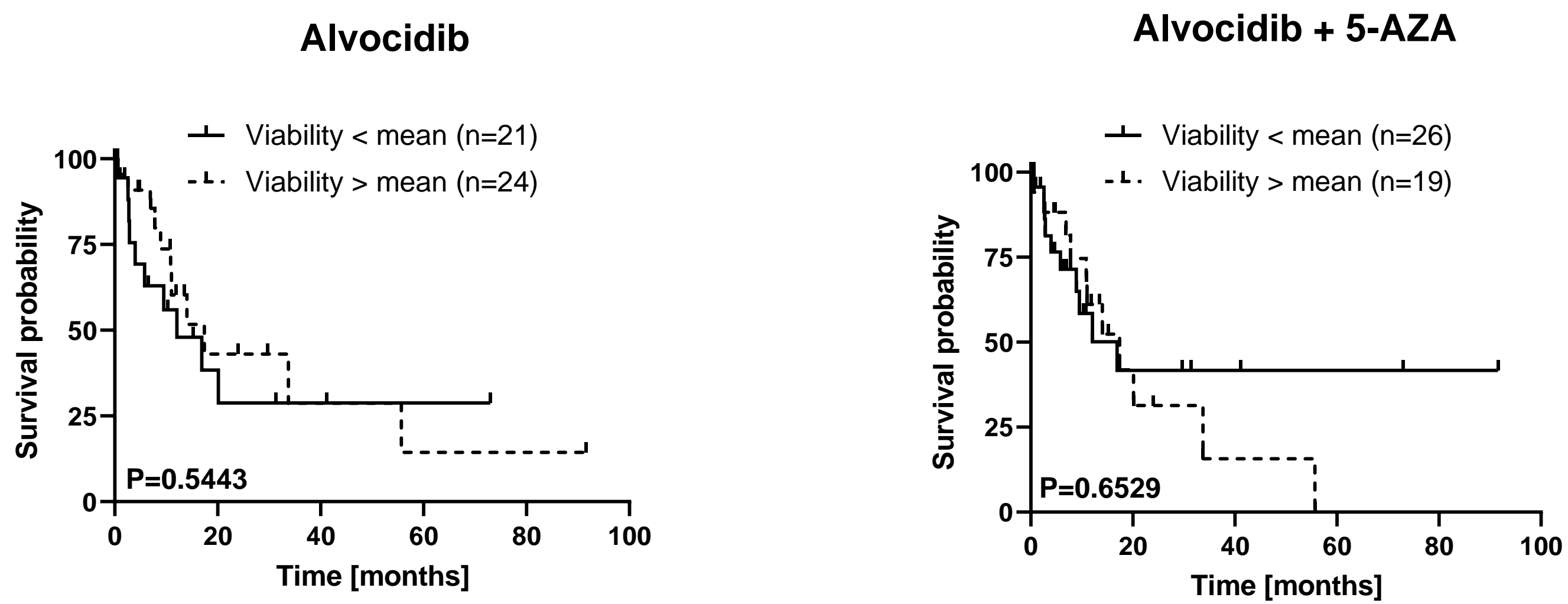


Supplementary Figure 2. Confirmation of DNMT3A W305fs mutation using Sanger sequencing in bone marrow MNCs and mesenchymal stromal cells (MSCs, germline control) of healthy control 2 (HC 2). Frameshift position in MNCs and corresponding nucleotide in MSCs are indicated by arrows.

Figure S3

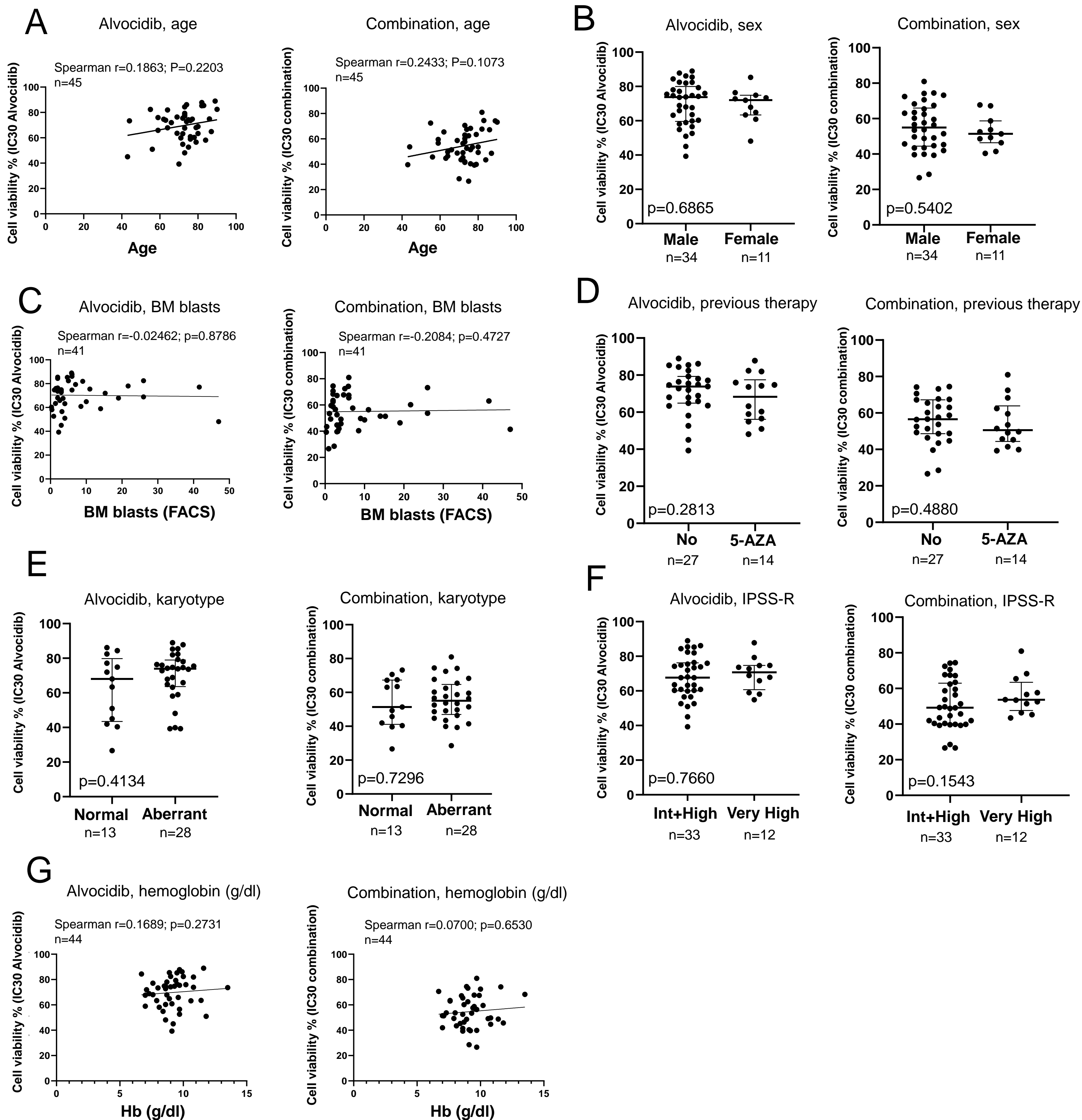
Supplementary Figure 3. Toxicity assessment of alvocidib + 5-AZA combination in vivo. NSGS mice were treated with 5-AZA (n=8), Alvocidib (n=8) their combination (n=9) or left untreated (n=10) for 37 days. **(A)** Body weights were measured every 3-4 days during the treatment; Blood counts including WBC **(B)**, RBC **(C)**, Hb **(D)** and PLT **(E)** were performed on the day 37 of treatment (day 50 post-transplantation), and sample size for each treatment group is indicated under the panels. For panel **(A)** the data are presented as mean \pm SD; for panels **B-E** Kruskal-Wallis test with Dunn's multiple comparisons was performed and medians are indicated.

Figure S4



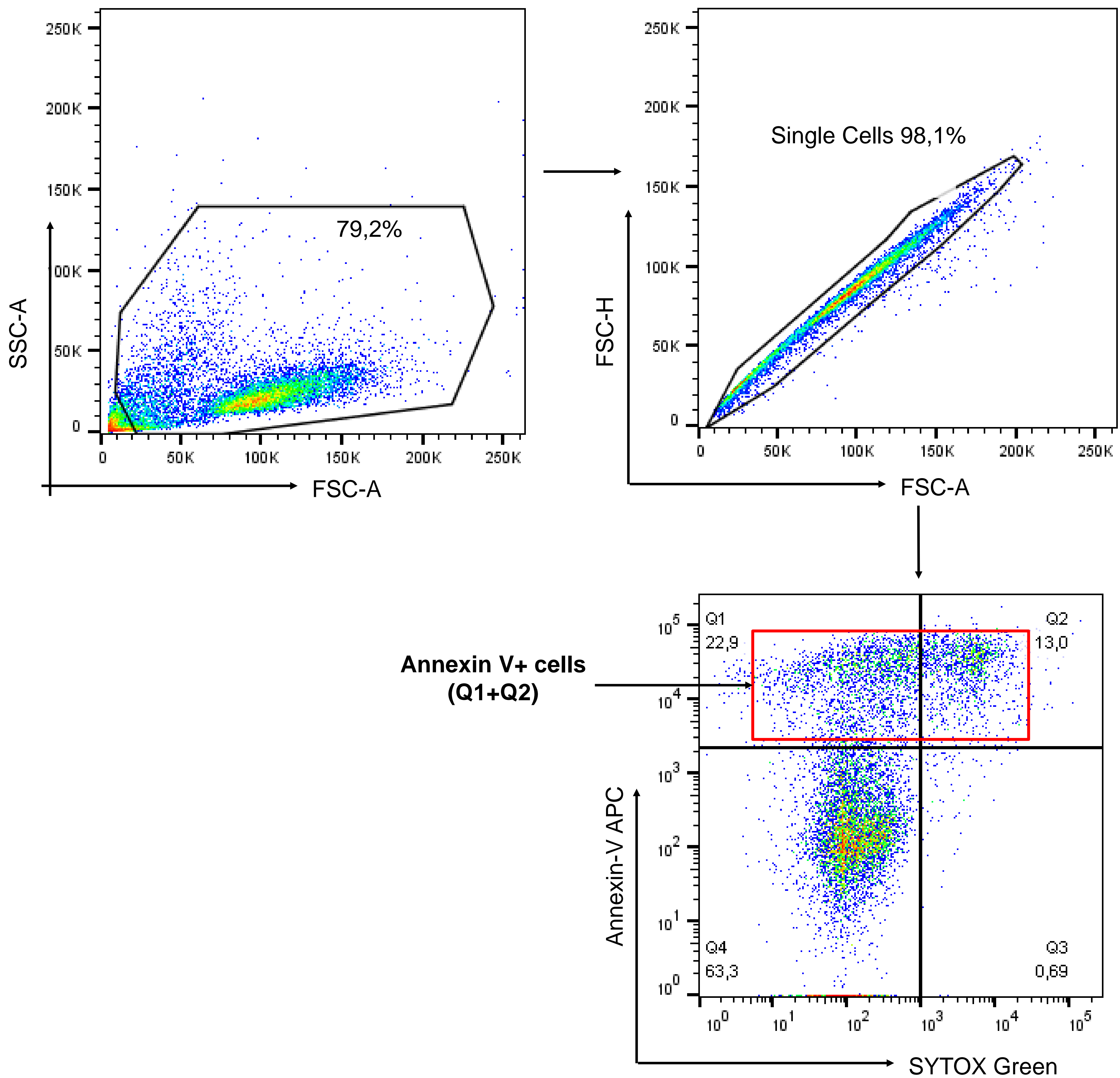
Supplementary Figure 4. The association of alvocidib and alvocidib + 5-AZA sensitivity *in vitro* with overall survival in n=45 MDS patients was assessed based on the mean cell viability in CTG assays. Kaplan-Meier curves were analyzed using log-rank test.

Figure S5



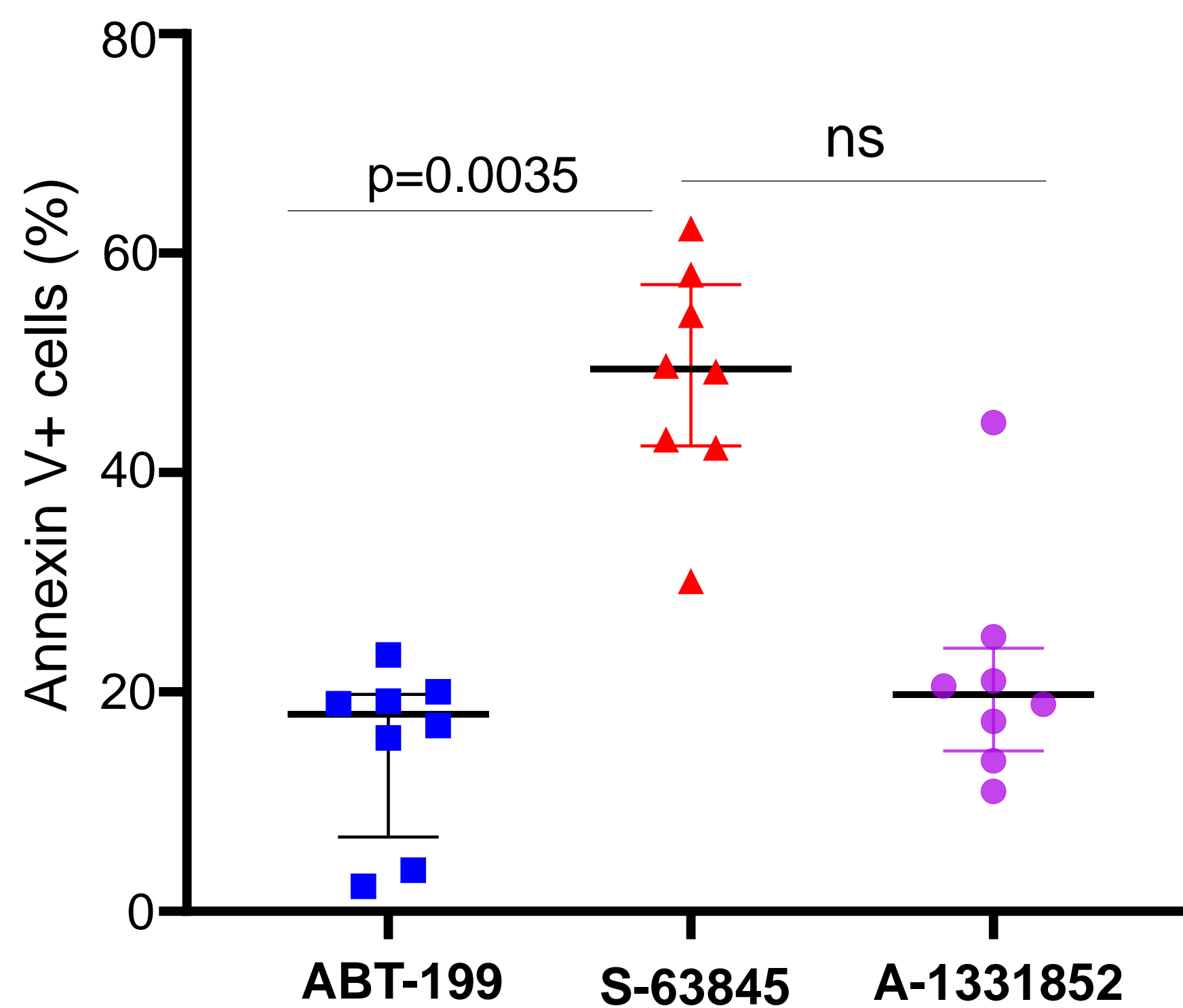
Supplementary Figure 5. The association of alvocidib and alvocidib + 5-AZA sensitivity with clinical characteristics of MDS patients: **(A)** Age, **(B)** Sex, **(C)** percentage of BM blasts, **(D)** Previous therapy, **(E)** Karyotype, **(F)** IPSS-R risk stratification and **(G)** hemoglobin at the time of BM puncture. Statistical analysis was performed using Spearman correlation test **(A, C, G)**. For panels **B, D, E, F** data are presented as median \pm IQR, Mann-Whitney U-test.

Figure S6



Supplementary Figure 6. Gating strategy for Annexin V apoptosis assay

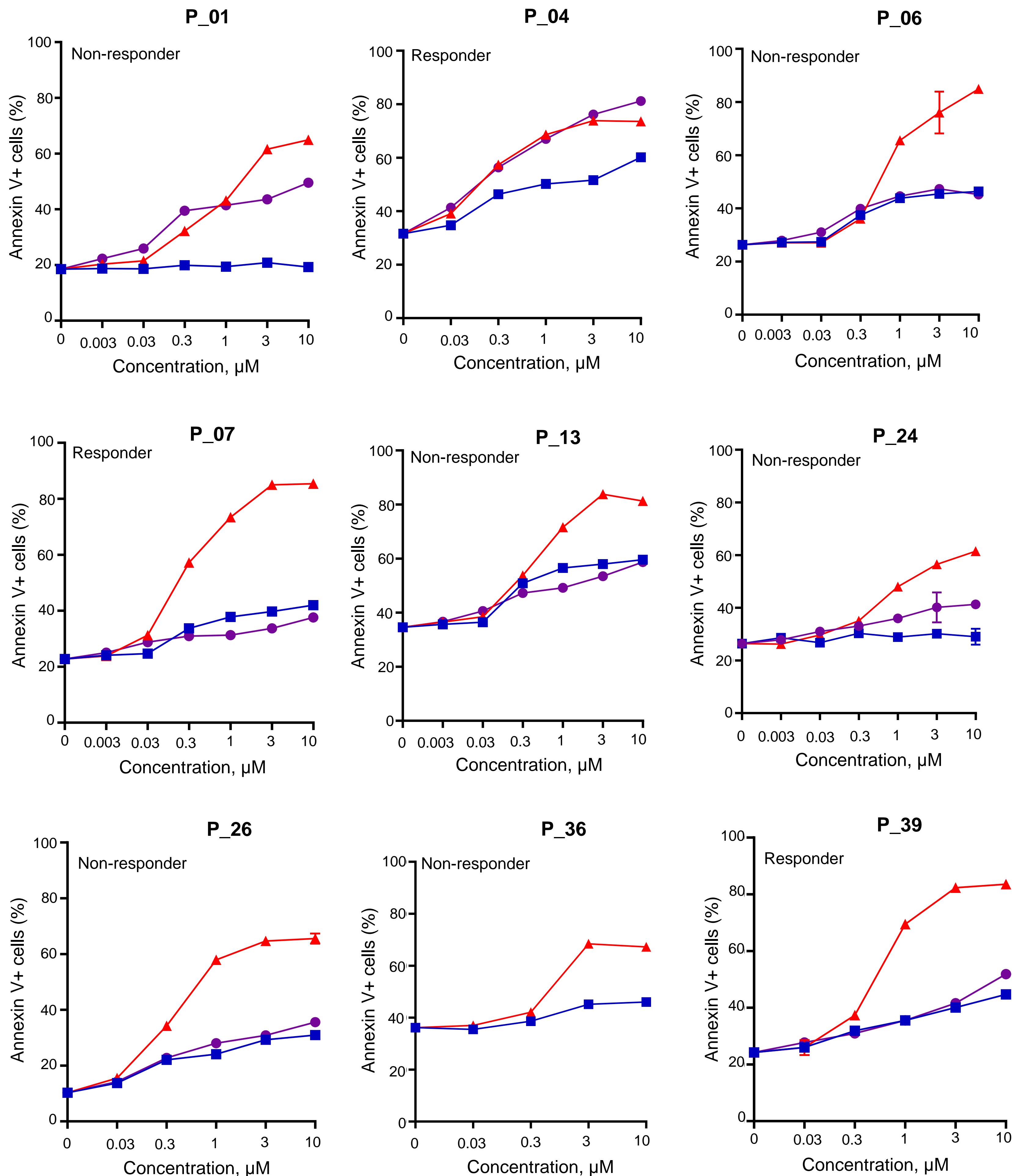
Figure S7



Supplementary Figure 7. Sensitivity of high-risk MDS samples to BH3 mimetics. *In vitro* expanded CD34+ cells of n=8 MDS patients were treated with BH3 mimetics S-63845, ABT-199 and A-1331852 for 24h followed by the assessment of apoptosis by flow cytometry using Annexin V; Friedman test with Dunn's multiple comparisons. The data are shown as median \pm IQR; ns – not significant.

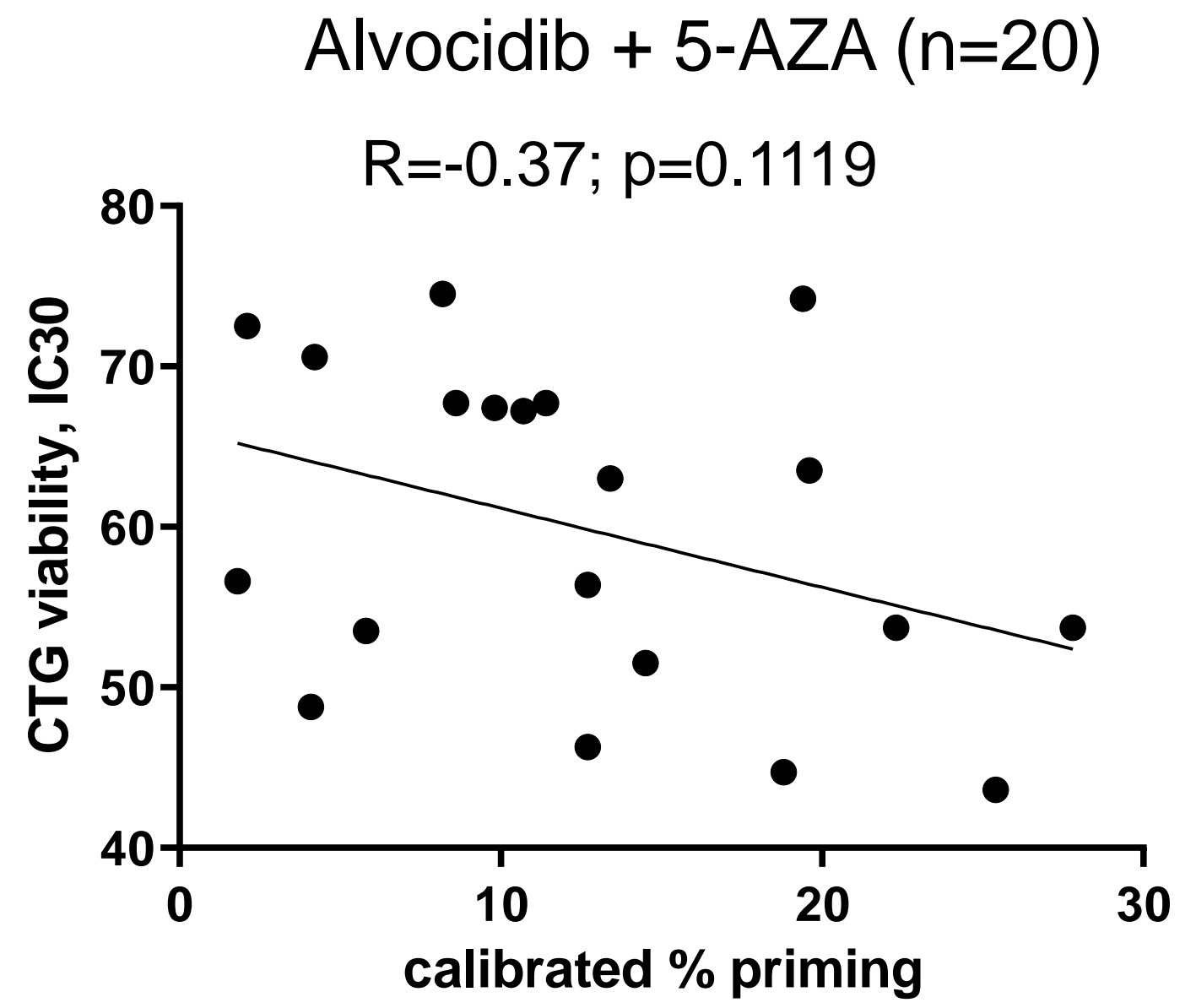
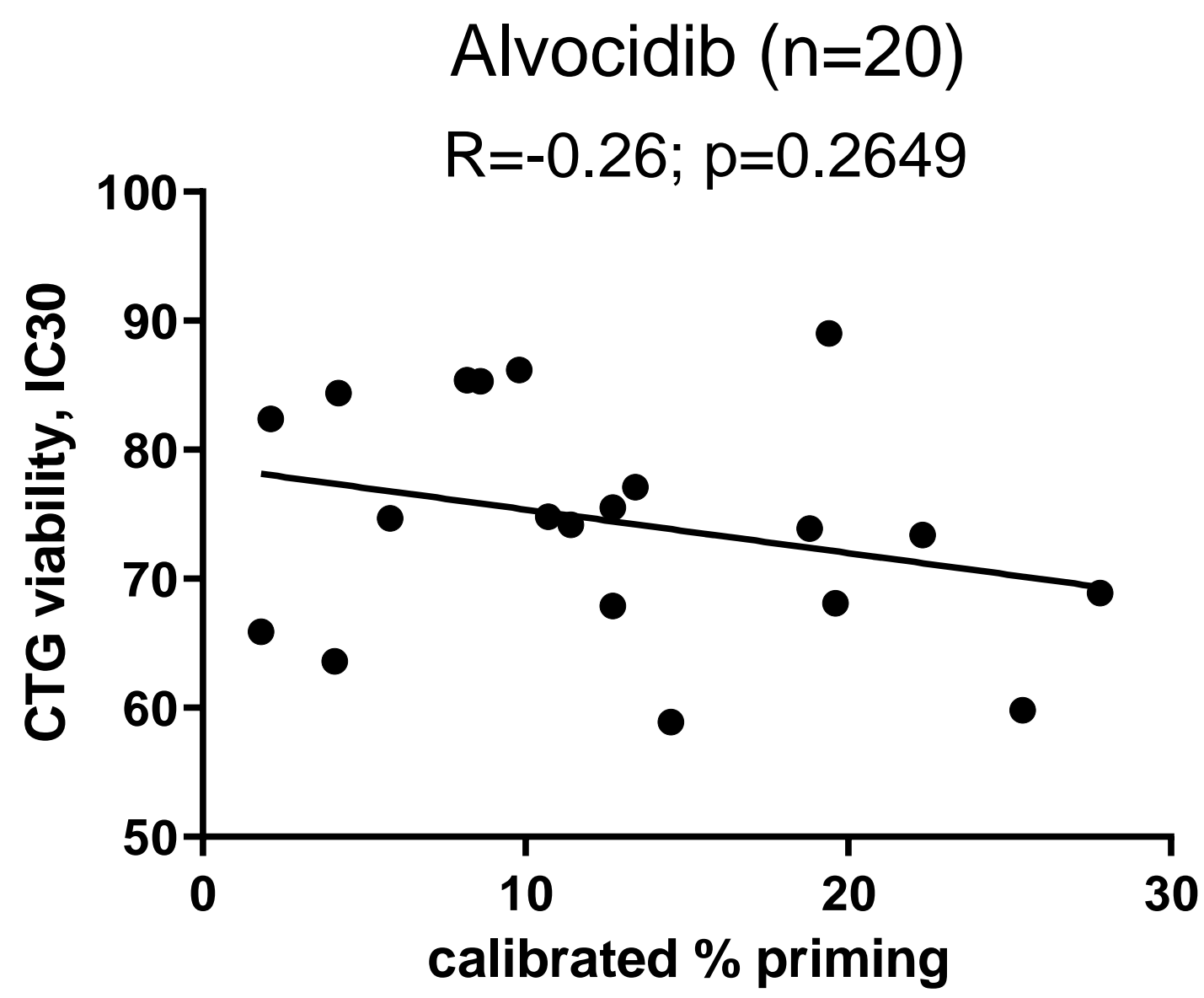
Figure S8

▲ S-63845 (MCL-1) ■ ABT-199 (BCL-2) ● A-1331852 (BCL-xL)



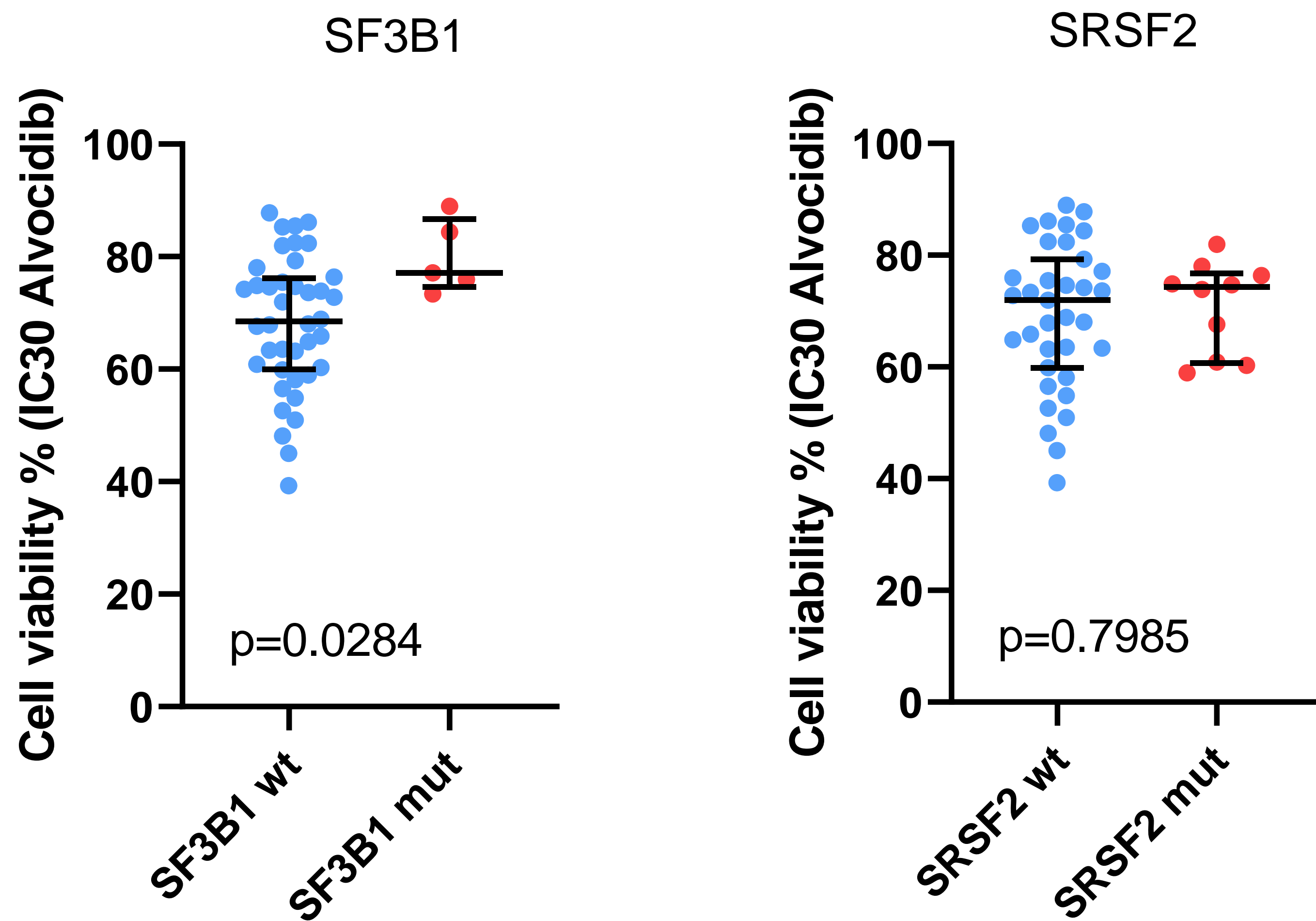
Supplementary Figure 8. The response of *in vitro* expanded CD34+ cells to BH3 mimetics S-63845, ABT-199 and A-1331852 was compared in n=9 high-risk MDS patients and evaluated as a percentage of annexin V+ positive cells using flow cytometry after 24h incubation with indicated drug concentrations. The data are mean \pm SD of n=2 technical measurement replicates.

Figure S9



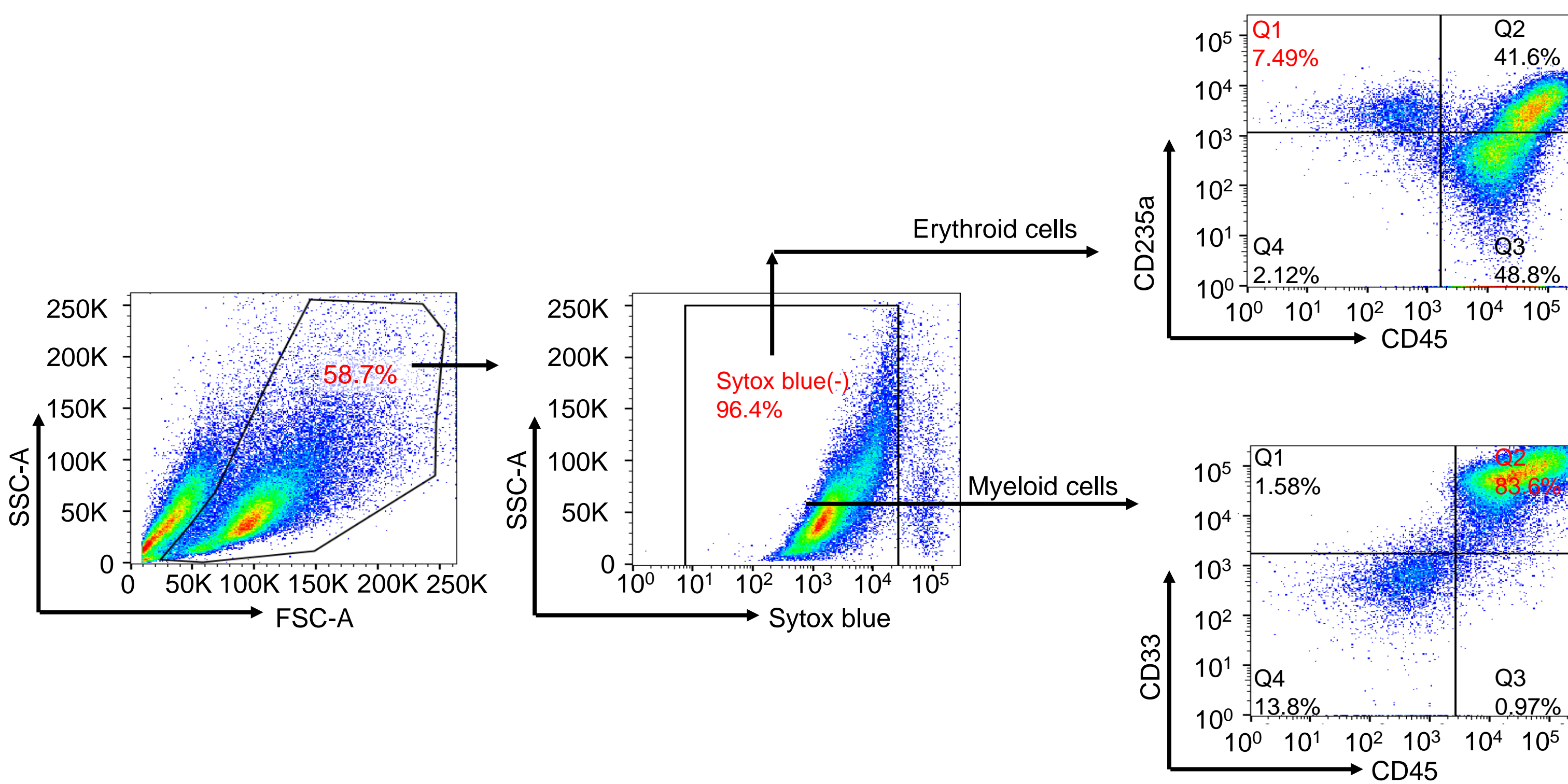
Supplementary Figure 9. Correlation between alvocidib and alvocidib + 5-AZA sensitivity in CTG assays and MCL-1 dependency (calibrated % priming) of patient MNCs was examined using n=20 MDS samples; Spearman correlation test.

Figure S10



Supplementary Figure 10. The association of cell viability in CTG assay after alvocidib treatment with the presence of SF3B1 and SRSF2 mutations for n=45 MDS samples; median \pm IQR, Mann-Whitney U-test.

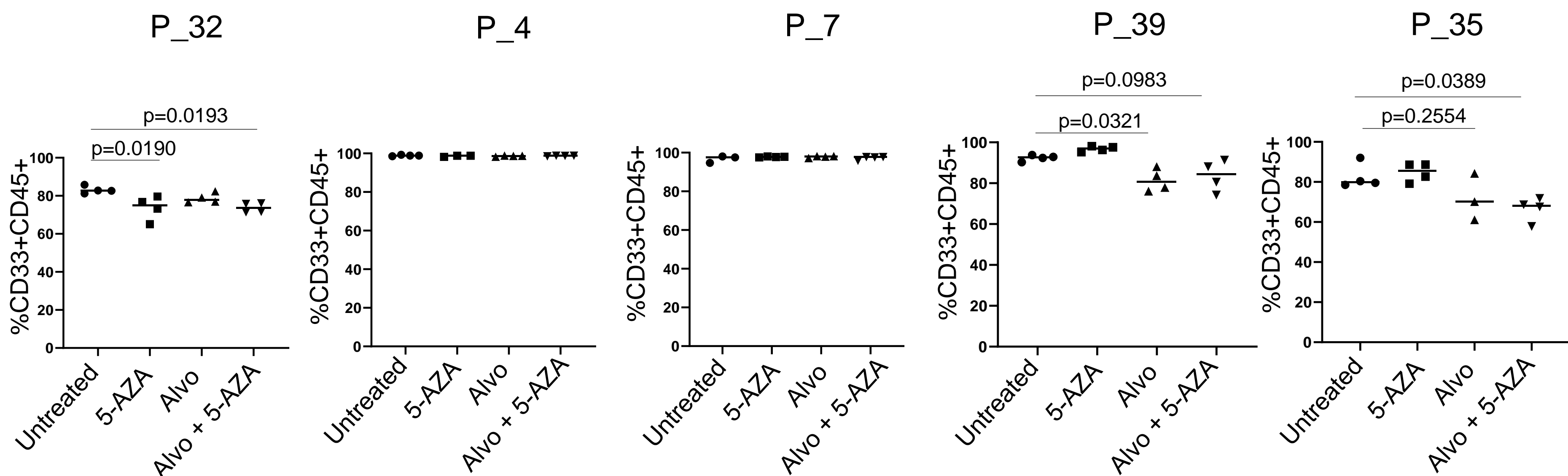
Figure S11



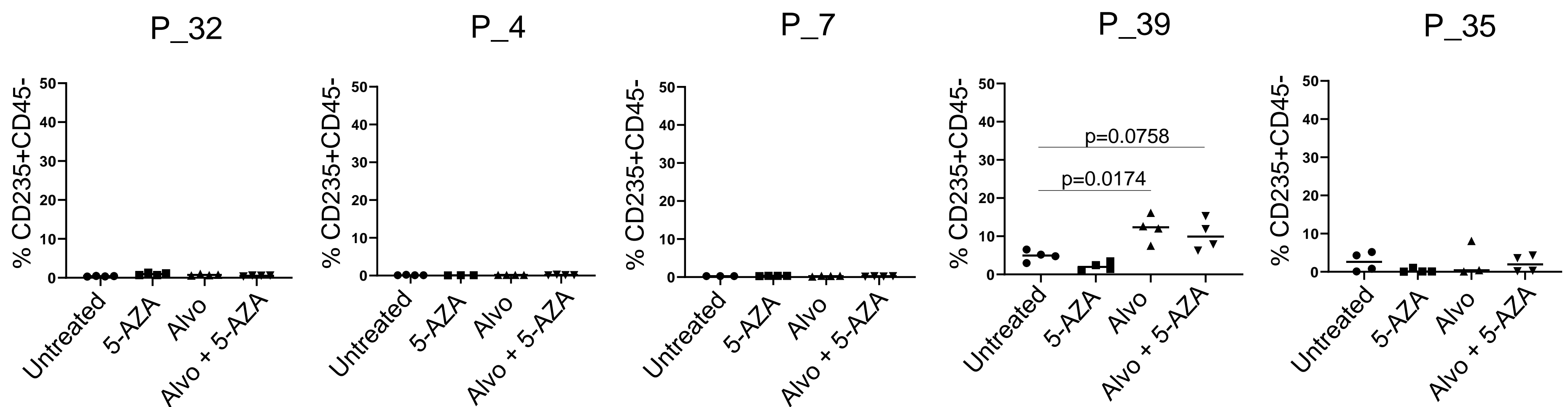
Supplementary Figure 11. Gating strategy for the detection of erythroid (CD235a+CD45-) and myeloid (CD45+CD33+) cells after colony-forming unit (CFU) assay

Figure S12

A. Myeloid differentiation



B. Erythroid differentiation



Supplementary Figure 12. The effect of 5-AZA, Alvocidib and Alvocidib + 5-AZA treatments on the differentiation capacity of MDS cells. CD34⁺ BM cells of n=5 high-risk MDS patients were treated with 5-AZA for 48, Alvocidib for 24h or their sequential combination (5-AZA for 48h followed by Alvocidib for 24h) and subjected to colony-forming unit (CFU) assay. Cells were harvested from CFU plates after 14 days and subjected to flow cytometry analysis to detect myeloid (CD33+CD45⁺) and erythroid (CD235a+CD45⁻) progenitors. The data were analyzed using one-way ANOVA with Tukey's multiple comparisons; medians are indicated for at least triplicates of CFU assay plates for each treatment condition.